# SSNV186 – the purpose of LBB condition and contact rubbing with X-FEM

**Summarized**

This test are of the contact validating the taking into account (by the continuous method [bib1]) on the lips of crack in the frame of the method X-FEM [bib2], when the LBB condition [bib3] [bib4] is not respected.

The contact/friction is treated by an algorithm of Augmented Lagrangian for the modelizations A with H and by an algorithm penalized for the modelizations I with K.

This test brings into play a parallelepipedic block in compression. The interface the beam is represented by a level set. The interface is right, NON-leaning and crosses the elements completely.

# 1 Problem of reference

Of the oscillations of contact pressures can appear in certain cases, in particular for structures where the interface cuts pentahedrons, under a non-uniform loading.

That is due to the non-observance of the LBB condition [bib3] [bib4]. This phenomenon of oscillations is comparable to that met of incompressibility [bib5]. Physically, in the case of the contact, that amount wanting to impose the contact in too many points of the interface (overstrained), making the system hyperstatic. To slacken it, it is necessary to restrict the space of the Lagrange multipliers, as that is done in [bib6] for the conditions of Dirichlet with X-FEM. Such algorithm present P0 segments, which slow down convergence. A good algorithm must minimize the appearance of such segments. The algorithm proposed by Moës [bib6] to reduce the oscillations is adapted to 3D case (algorithm version 1). This algorithm was the object of an improvement to make it more physical and more effective (algorithm version 2). A comparison of the two versions is carried out.

It should be noted that these parasitic oscillations are not reproducible in the current version of Code_Aster: one of the two algorithms is systematically selected (the 2 is used by default), and even an overload of the code to use some no would bring a null pivot. We illustrate them in this documentation by results resulting from another formulation (formulation with the edges [bib7]), now reabsorbed.

For horizontally cut hexahedrons or quadrangles, there are no P0 segments.

## 1.1 Geometry

the structure is a right at square base and healthy parallelepiped. Dimensions of the block are: $LX=5\,m$ , $LY=20\,m$ and $LZ=20\,m$ . It does not comprise any crack [Figure 1.1-1].

The interface is introduced by functions of levels (level sets) directly into the command file using operator `DEFI_FISS_XFEM` [U4.82.08]. The interface is present within structure by the means of its representation by the level sets. The level set norm ( $LSN$ ) makes it possible to define an interface planes NON-leaning which crosses the elements completely, by the following equation:

$$LSN = Z - 17.5$$ **éq 1.1-1**

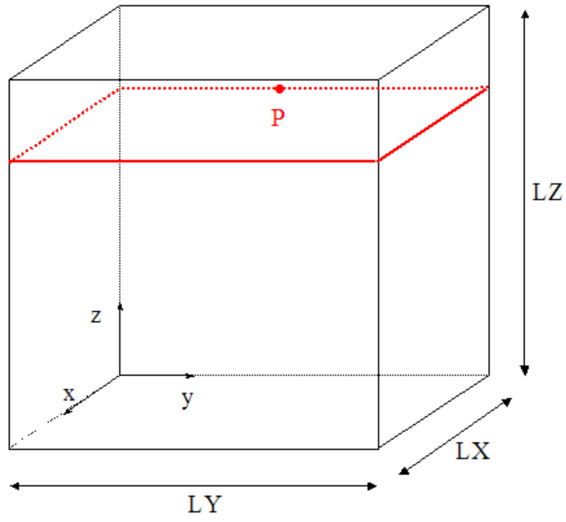


**Figure 1.1-1 : Geometry and positioning of the interface**

## 1.2 Properties of the material

Modulus Young: $E = 1000\,Pa$ .
Poisson's ratio: $\nu = 0$ .

## 1.3 Boundary conditions and loadings

the lower face is clamped.
The upper face is subjected to a parabolic pressure having for statement:

$$pression = \left(100 - \frac{(Y-10)^2}{2}\right)\frac{E}{10^6}\,Pa$$ **éq 1.3-1**

displacements along the axes $x$ and $y$ are blocked for the nodes of the upper surface.

## 1.4 Bibliography

1.Massin P., Ben Dhia H., Zarroug Mr.: Elements of contacts derived from a continuous hybrid formulation, Handbook of reference of *the Code_Aster*, [R5.03.52]

2.Massin P., Geniaut S.: Method X-FEM, Handbook of reference of *the Code_Aster*, [R7.02.12]

3.Babuška I.: The finite element method with lagrangian multipliers, Numerische Math 20,179 - 192, 1973

4.Barbosa H., Hugues T.: Finite element method with lagrange multipliers one the boundary. Circumventing the Babuška-Brezzi condition, comp. Meth. Applied Mech Engrg. 85 (1), 109 - 128, 1991

5.Vault D., Bathe K.J.: The Inf-sup test, Computers & Structures 47 (4/5), 537-545, 1993

6. Moës N., Béchet E., Peaty Mr.: Imposing Dirichlet boundary conditions in the extended finite element method, Int. J. Numer. Meth. Engng, 2006, vol. 67(12), 1641-1699.

7. Géniaut S., Massin P., Moës N., A stable 3D contact formulation using X-FEM, European Newspaper of Computational Mechanics, Vol.16, n°2, Pages 259-276, 2007.

# 2 Modelization a: hexahedrons (version 2)

In this modelization, the mesh considered comprises only hexahedrons. This modelization is used as reference for the others, because this case does not present P0 segments. Indeed, in the case of the hexahedrons cut by an interface parallel to the sides, the number of contact pressures (one by cut edge) is compatible with the discretization of the field of displacement [bib1] [bib2].

## 2.1 Characteristics of the mesh

the problem is invariant following the axis $Ox$. In order to limit the computing time, the mesh considered here comprises one element along this axis. The structure is then modelled by a regular mesh composed $1\times20\times20$ HEXA8 to see [Figure 2.1-1].

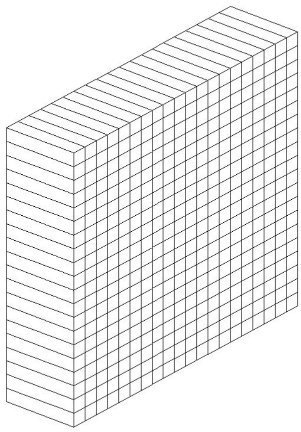

**Figure 2.1-1 : Mesh of hexahedrons**

This mesh is composed of linear finite elements. In the frame of the continuous method [bib1] with X-FEM [bib2], the unknowns of contact are carried by the nodes tops.

## 2.2 Features tested

One uses the diagram of integration Gauss points reduced to 4 per facet of contact.
Friction is taken into account and the contact is active as of the 1st iteration of active stresses.

## 2.3 Quantities tested and results

One tests the value of the contact pressure at the point $P$ of coordinates $(0,10,17.5)$. This value is used as reference for the other modelizations.

$$\lambda=-9.52844\,10^{-2}\,Pa$$

# 3 Modelization D: pentahedrons (version 2)

## 3.1 Characteristic of the mesh

The mesh is identical to that of the modelization B.

## 3.2 Functionalities tested

One uses the diagram of integration Gauss points reduced to 4 per facet of contact.
Friction is taken into account and the contact is active as of the 1st iteration of active stresses.
The algorithm aiming at restricting the space of the Lagrange multipliers is the n°2.

## 3.3 Quantities tested and results

One tests the value of the contact pressure at the point $P$ of coordinates $(0,10,17.5)$ .

| Identification | Reference | *Aster* | % difference |
|---|---|---|---|
| Not $P$ | $-9.52844\,10^{-2}$ | $-9.5188\,10^{-2}$ | 0.10 |

## 3.4 Comments

This modelization shows that the algorithm version 2 makes it possible to reduce the oscillations efficiently. It is observed that the algorithm version 2 tends to introduce approximations $P1$ per pieces of contact pressures on the interface, which makes it more precise than the version1 (see also it [Figure 5.2-1] and it [Figure 5.2-2]).

# 4 Modelization E: tetrahedrons (algorithm version 1)

This test brings into play a free mesh made up of tetrahedrons. In order to reduce the number of elements and thus the computing time, the length of structure along the axis $Ox$ is $LX=1\ m$ .

## 4.1 Characteristics of the mesh

The mesh considered is a free mesh carried out with GMSH. It consists of 3629 TETRA4. [Figure 4.1-1] the mesh in the plane represents $Oyz$ . The interface is traced there only at ends of visualization.

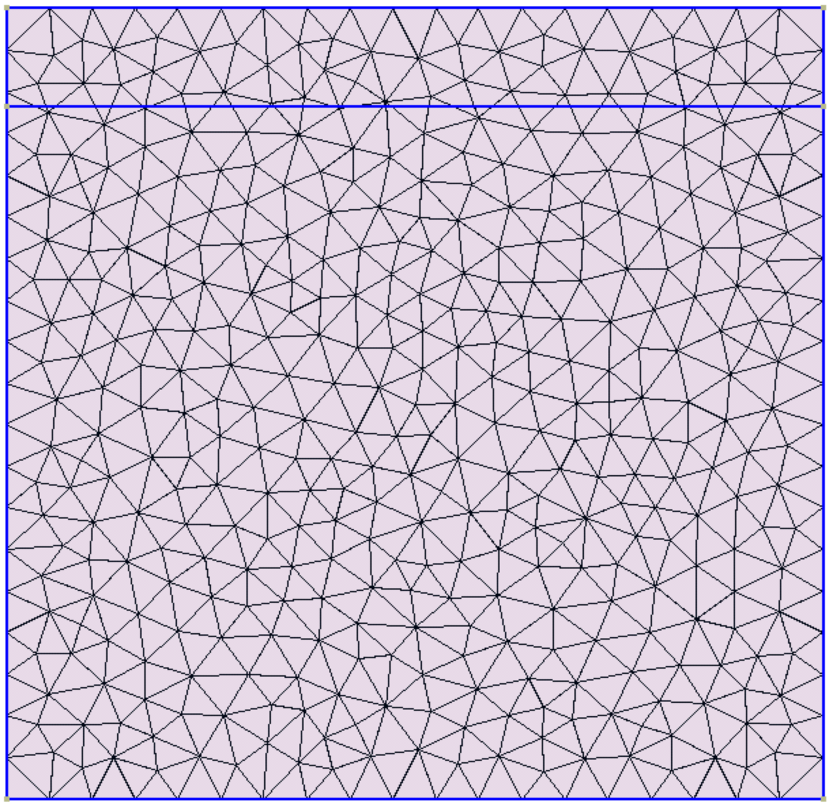

**Figure 4.1-1 : Free mesh**

## 4.2 Boundary conditions and loadings

the lower face is clamped.
The upper face is subjected to a uniform pressure:

$$pression=100\frac{E}{10^6}Pa$$ **éq 4.2-1**

displacements along the axes $x$ and $y$ are blocked for the nodes of the upper surface.

## 4.3 Features tested

One uses the diagram of integration Gauss points reduced to 4 per facet of contact.
The contact is active as of the 1st iteration of active stresses but friction is not taken into account
the algorithm aiming at restricting the space of the Lagrange multipliers is the n°1.

## 4.4 Quantities tested and results

One tests the value of contact pressures for all the points of the interface. The analytical solution is quite simply:

$$\lambda=\sigma_{zz}=-pression$$ **éq 4.4-1**

| **Identification** | **Reference** | ***Aster*** | **% difference** |
|---|---|---|---|
| `MAX (LAGS_C)` | -0.1 | 0.0979 | -2.08 |
| `MIN (LAGS_C)` | -0.1 | -0.1016 | 1.62 |

to test all the points of contact into only one times, one tests the minimum and the maximum of column.

## 4.5 Comments

This test makes it possible to validate the robustness of the algorithm of restriction of the space of the Lagrange multipliers of pressure, in a case of free mesh in 3D. Even on a structure subjected to constant pressure, the algorithm is essential bus of the oscillations of contact pressures can appear (it is the case here if the algorithm is not activated).

# 5 Summaries of the results 3D

## 5.1 Summarized

In the frame of the method X-FEM, it was shown that, without particular processing, a structure with a grid with pentahedrons subjected to a non-uniform loading can have strong oscillations of contact pressures, as shows it the second curve of [Figure 5.2-1]), realized with a different formulation [bib7], now reabsorbed in Code_Aster, for which the absence of algorithm of restriction did not actuate a null pivot. The same structure with a grid with hexahedrons subjected to the same loading does not have such oscillations (modelization A being used as reference).

One proposed two algorithms allowing to reduce these oscillations significantly. The first (third curve of [Figure 5.2-1]) seems less precise than the second (modelization D).

Moreover even under uniform loading, of the oscillations can appear and it is essential to use an algorithm of reduction of the space of the Lagrange multipliers of pressure (modelization E).

## 5.2 Curves of comparison

It [Figure 5.2-1] gathers the curves of contact pressures along the axis $Oy$ for the first 4 modelizations presented. It is noticed that the oscillations for the modelization B are so strong that in certain points the value of the contact pressure becomes positive, which would like to say that there is separation of the interface. The two algorithms allow a visible reduction of the oscillations, and one finds the curve of reference obtained with the mesh of hexahedrons.

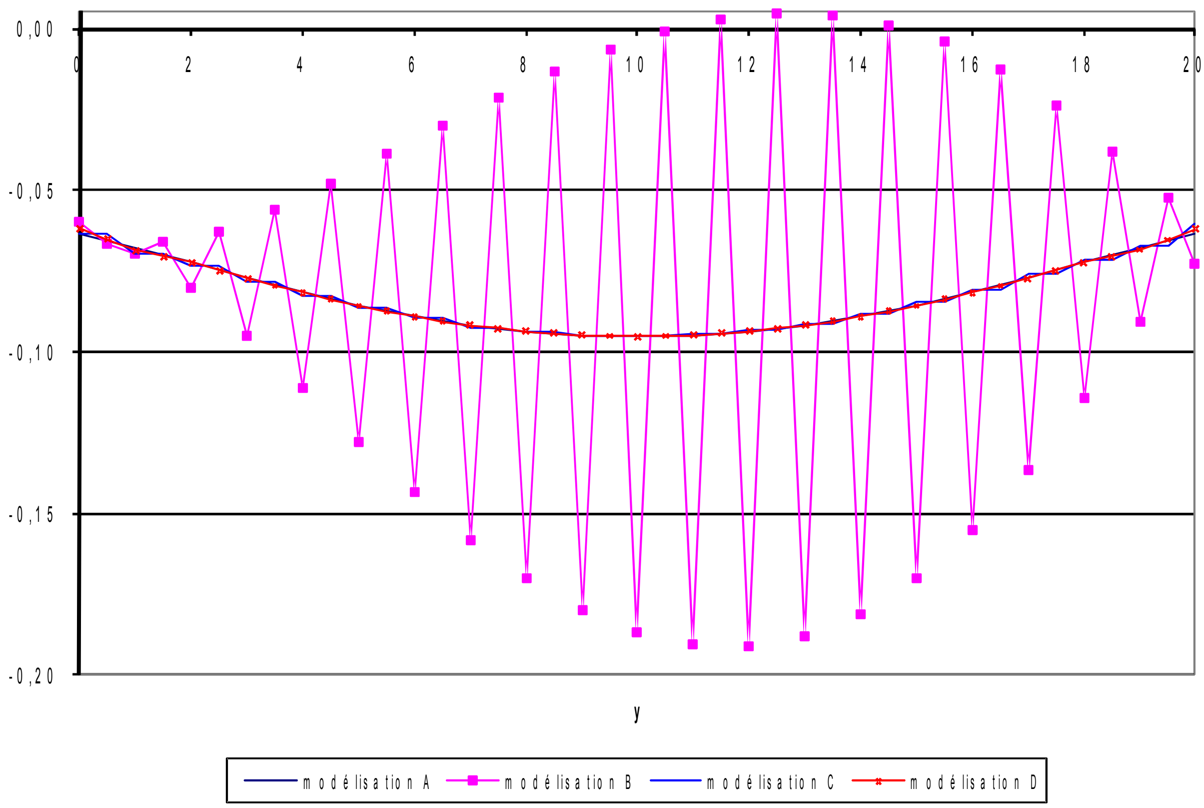


**Figure 5.2-1 : Comparison of contact pressures following the modelizations**

It [Figure 5.2-2] compares in details the effects of the two algorithms. It is noticed that the first often implies constant contact pressures per pieces, whereas the second tends to linearize the pressures. It is obvious that such differences are reduced by refining the mesh.

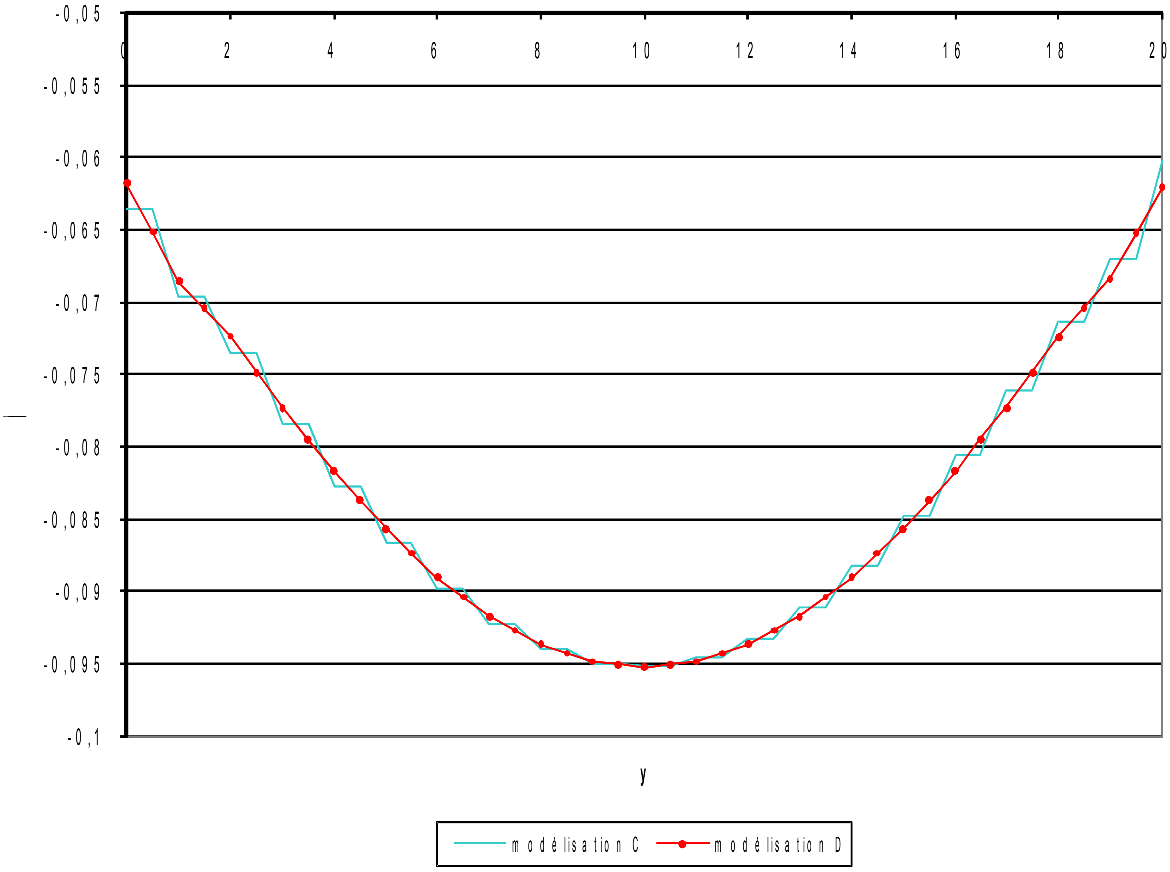


**Figure 5.2-2 : Comparison of the 2 algorithms**

# 6 Modelization F: quadrangles 2D

This modelization is the equivalent in 2D of the modelization A (reference). This case does not have oscillations of contact pressures. Just like in the modelization A, the quadrangles are cut by an interface parallel to the edges. There are then no P0 segments.

## 6.1 Characteristics of the mesh

the structure is then modelled by a regular mesh composed of $20\times20$ QUAD4 (See [Figure 6.1-1]).

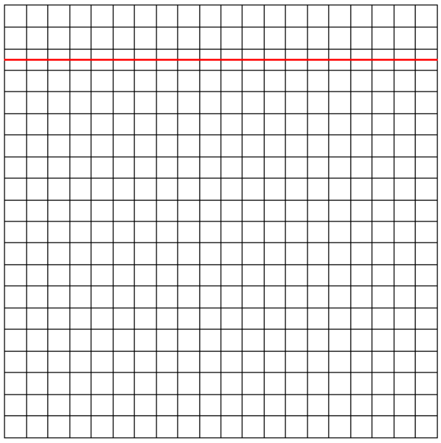

**Figure 6.1-1 : Mesh of quadrangles**

## 6.2 Features tested

friction is taken into account and the contact is active as of the 1st iteration of active stresses.
The algorithm aiming at restricting the space of the Lagrange multipliers is number 2.

## 6.3 Quantities tested and results

One tests the value of the contact pressure at the point $P$ of coordinates $(10,17.5)$ .

| Identification | Reference | *Aster* | % difference |
|---|---|---|---|
| Not $P$ | $-9.52844\,10^{-2}$ | $-9.52844\,10^{-2}$ | $2.41\,10^{-4}$ |

## 6.4 Comments

This case test makes it possible A to find the values of reference of contact pressures calculated in the modelization, and to check that in the case of quadrangles cut their sides parallel to, these contact pressures do not present P0 segments (see [Figure 9.2-1]).

# 7 Modelization G: triangles (algorithm version 1)

## 7.1 Characteristic of the mesh

the structure is modelled by a regular mesh composed of triangles. The test is the equivalent in 2D of the modelization B (See [Figure 7.1-1]).

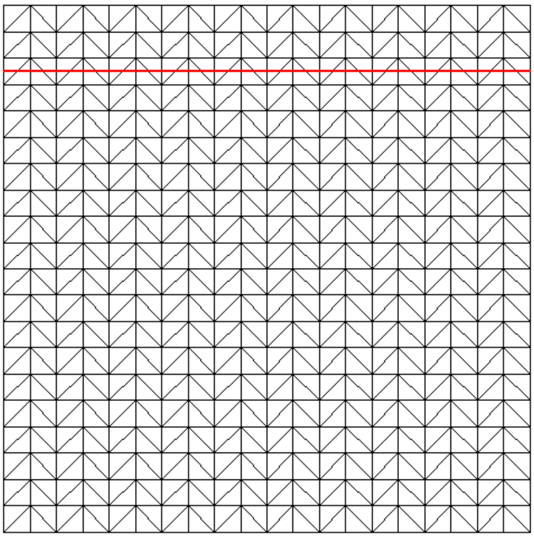

**Figure 7.1-1 : Mesh of triangles**

## 7.2 Features tested

friction is taken into account and the contact is active as of the 1st iteration of active stresses.
The algorithm aiming at restricting the space of the Lagrange multipliers is the n°1.

## 7.3 Quantities tested and results

One tests the value of the contact pressure at the point $P$ of coordinates $(10,17.5)$ .

| Identification | Reference | *Aster* | % difference |
|---|---|---|---|
| Not $P$ | $-9.52844\,10^{-2}$ | $-9.59082\,10^{-2}$ | 0.655 |

## 7.4 Comments

This modelization shows that the algorithm set up makes it possible to reduce the oscillations effectively. (see [Figure 9.2-1]).

# 8 Modelization H: triangles (algorithm version 2)

## 8.1 Characteristic of the mesh

The mesh is identical to that of the modelization G.

## 8.2 Functionalities tested

friction is taken into account and the contact is active as of the 1st iteration of active stresses.
The algorithm aiming at restricting the space of the Lagrange multipliers is the n°2.

## 8.3 Quantities tested and results

One tests the value of the contact pressure at the point $P$ of coordinates $(10,17.5)$ .

| **Identification** | **Reference** | ***Aster*** | **% difference** |
|---|---|---|---|
| Not $P$ | $-9.52844\,10^{-2}$ | $-9.59082\,10^{-2}$ | 0.655 |

## 8.4 Comments

This modelization shows that in 2D, the algorithm version 2 has a behavior very close to that of version 1. Indeed, put except for the first contact pressures measured on the left of the mesh, the actual values identical, curved are and the obtained with the two algorithms are recovered almost completely. (see [Figure 9.2-1]).

# 9 Summaries of the results 2D

## 9.1 Summarized

It, initially, was checked that the behavior of structure of reference (modelization A) could be found in 2D (modelization F). After having observed the phenomenon of oscillations in 2D, one tested on cases in 2D the two algorithms which make it possible to reduce these oscillations in 3D.

The two algorithms tested in the modelizations G and H give, in 2 dimensions, of the very close results, and make it possible consequently to reduce the oscillations introduced by the mesh.

## 9.2 Curves of comparison

It [Figure 9.2-1] represents the curves of contact pressures along axis OX for the 3 modelizations in 2D presented. It is noticed that the curves representative of the two algorithms are recovered almost completely. The two algorithms are thus about as efficient one as the other in 2D. It make it possible nevertheless to reduce the oscillations effectively.

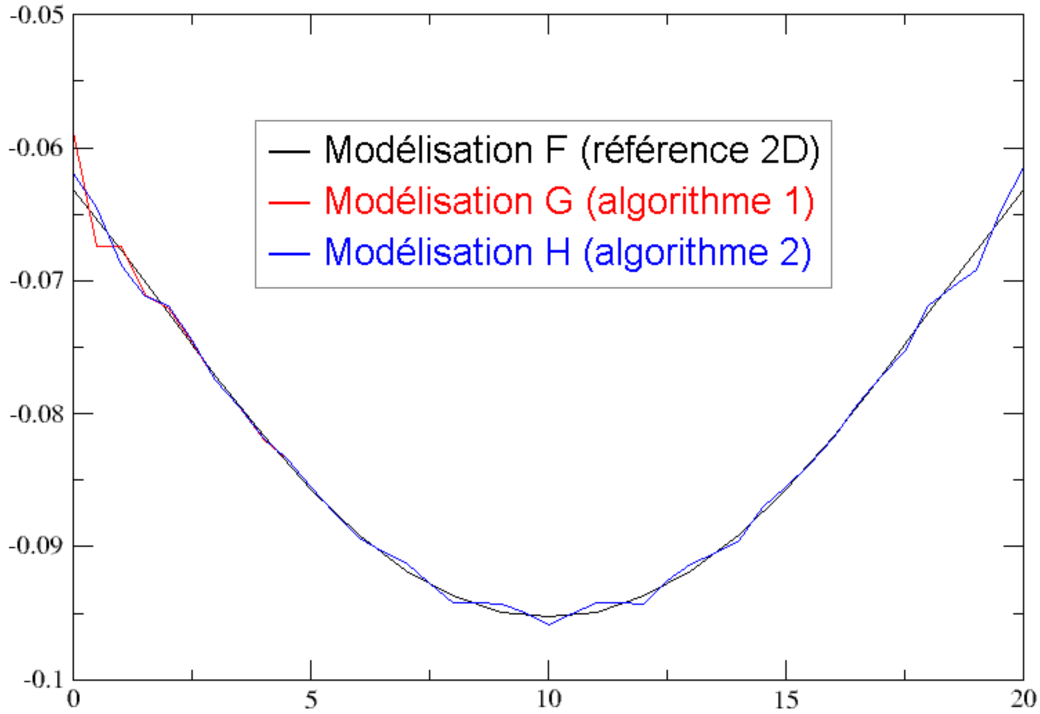


**Figure 9.2-1 : Comparison of contact pressures following the modelizations 2D.**

It is it should be noted that a refinement of mesh increases obviously the accuracy of the got results.

# 10 Modelization I: pentahedrons (algorithm version 2), method penalized

## 10.1 Characteristic of the mesh

The mesh is identical to that of the modelization B.

## 10.2 Functionalities tested

One uses the diagram of integration Gauss points reduced to 4 per facet of contact.
Friction is taken into account and the contact is active as of the 1st iteration of active stresses.
The algorithm aiming at restricting the space of the Lagrange multipliers is the n°2.

## 10.3 Quantities tested and results

One tests the value of the contact pressure at the point $P$ of coordinates $(0,10,17.5)$.

| Identification | Reference | *Aster* | % difference |
|---|---|---|---|
| Not $P$ | $-9.52844\,10^{-2}$ | $-9.528856\,10^{-2}$ | $4.4\,10^{-3}$ |

## 10.4 Comments

One B finds results comparable to those of the modelization where the contact algorithm/friction was the Augmented Lagrangian one, and this, on all contact surface (see [Figure 26.2.1]).

# 11 Modelization J: tetrahedrons (algorithm version 1), penalized method

This test brings into play a free mesh made up of tetrahedrons. In order to reduce the number of elements and thus the computing time, the length of structure along the axis $Ox$ is $LX=1\,m$.

## 11.1 Characteristics of the mesh

The mesh is identical to that of the modelization E.

## 11.2 Boundary conditions and loadings

the lower face is clamped.
The upper face is subjected to a uniform pressure:

$$pression=100\frac{E}{10^6}Pa$$ **éq 11.2-1**

displacements along the axes $x$ and $y$ are blocked for the nodes of the upper surface.

## 11.3 Features tested

One uses the diagram of integration Gauss points reduced to 4 per facet of contact.
The contact is active as of the first iteration of active stresses.
The algorithm aiming at restricting the space of the Lagrange multipliers is the n°1.
One tests here the method penalized to treat the contact/friction.

## 11.4 Quantities tested and results

One tests the value of contact pressures for all the points of the interface. The analytical solution is quite simply:

$$\lambda=\sigma_{zz}=-pression$$ **éq 11.4-1**

| Identification | Reference | *Aster* | % difference |
|---|---|---|---|
| `MAX (LAGS_C)` | -0.1 | -0.100000364 | 3.6 10-4 |
| `MIN (LAGS_C)` | -0.1 | -0.09999551 | 4.5 10-3 |

to test all the points of contact into only one times, one tests the MINIMUM and the maximum of column.

## 11.5 Comments

One E finds results comparable to those of the modelization where the contact algorithm/friction was the Augmented Lagrangian one.

# 12 Modelization K: triangles (algorithm version 1), method penalized

## 12.1 Characteristic of the mesh

The mesh is identical to that of the modelization G.

## 12.2 Functionalities tested

friction is taken into account and the contact is active as of the first iteration of active stresses.
The algorithm aiming at restricting the space of the Lagrange multipliers is the n°1.
One tests here the method penalized to treat the contact/friction.

## 12.3 Quantities tested and results

One tests the value of the contact pressure at the point $P$ of coordinates (10, 17.5).

| Identification | Reference | *Aster* | % difference |
|---|---|---|---|
| Not $P$ | $-9.52844\,10^{-2}$ | $9.5574\,10^{-2}$ | $0.30$ |

## 12.4 Comments

One G finds results comparable to those of the modelization where the contact algorithm/friction was the Augmented Lagrangian one, and this, on all contact surface (see [Figure 26.2.2]).

# 13 Summaries of the results of method penalized

## 13.1 Summarized

One showed that the penalized method made it possible to satisfy the LBB condition as well as the method of the Augmented Lagrangian one.

## 13.2 Curves of comparison

Figures 26.2.1 and 26.2.2 show the profile of contact pressure along the interface when one uses the penalized method and the method of Augmented Lagrangian. The results of the modelizations A and F are given as reference. It is noted that it has there very little difference between the results of the two methods.

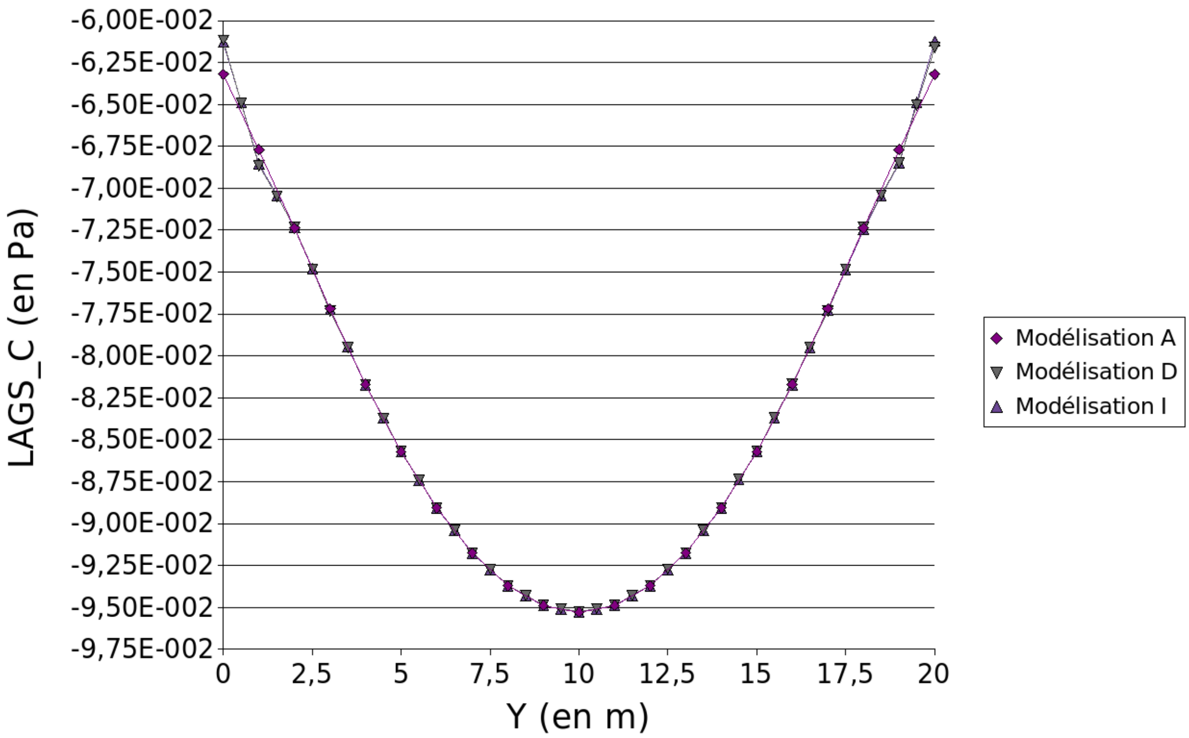


**Figure 13.2-1: Comparison of the method of Augmented Lagrangian and the method penalized in 3D.**

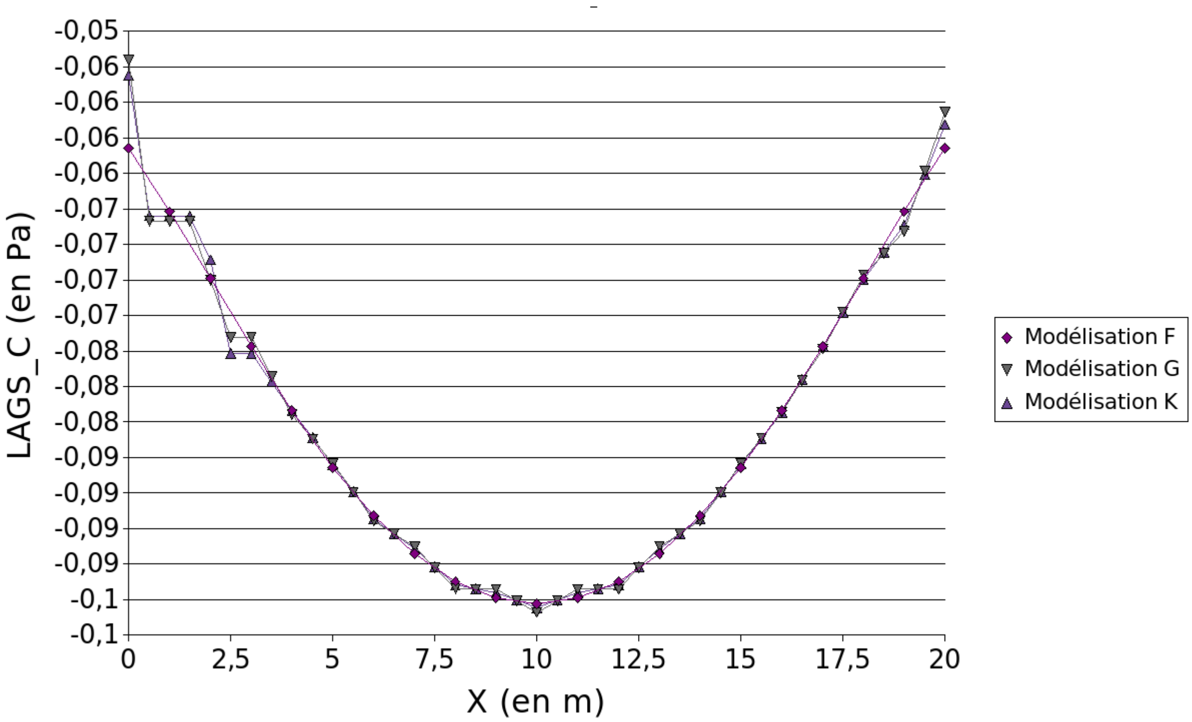


**Figure 13.2-2: Comparison of the method of Augmented Lagrangian and the method penalized in 2D.**

# 14 Modelization L: pyramids (algorithm version 2)

## 14.1 Characteristic of the mesh

The mesh in linear elements consists of hexahedrons, tetrahedrons and pyramids. The crack illustrated in blue on Figure 14.1-1 part of the pyramids and tetrahedrons in their medium.

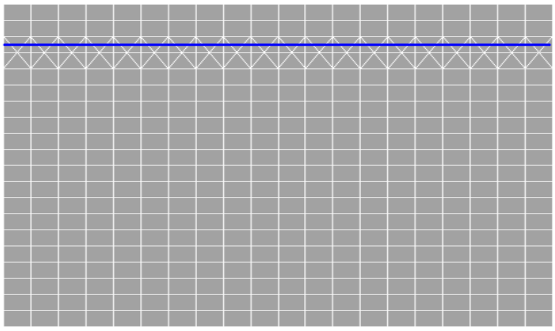

**Figure 14.1-1: Mesh of hexahedrons, tetrahedrons and pyramids**

## 14.2 Features tested

friction is taken into account and the contact is active as of the first iteration of active stresses. Unknown contact pressures are put at the nodes of the elements. The algorithm aiming at restricting the space of the Lagrange multipliers is the n°2. The elements pyramid here are tested.

## 14.3 Quantities tested and results

One tests the value of the respective coordinate and contact pressure $P1$ $P2$ at the point $(0,10,17.)$ and $(0,10,18.)$. These nodes are the tops of the edge passing by the point $P$ $(0,10,17.5)$.

| Identification | Reference | *Aster* | % difference |
|---|---|---|---|
| Points $P1$ and $P2$ | $-9.52844\,10^{-2}$ | $-9.52640\,10^{-2}$ | 0.0351 |

## 14.4 Curves in comparison

It [Figure 14.4-1] represents the curves of contact pressures along the axis $Oy$ with $x=0$ for the modelizations A and L. One took the values in $z=17$ for the modelization M since there is no point in $z=17.5$ as for modelization A. One notices all the same that the curve of the modelization L follows well the curve of reference obtained with the mesh of hexahedrons.

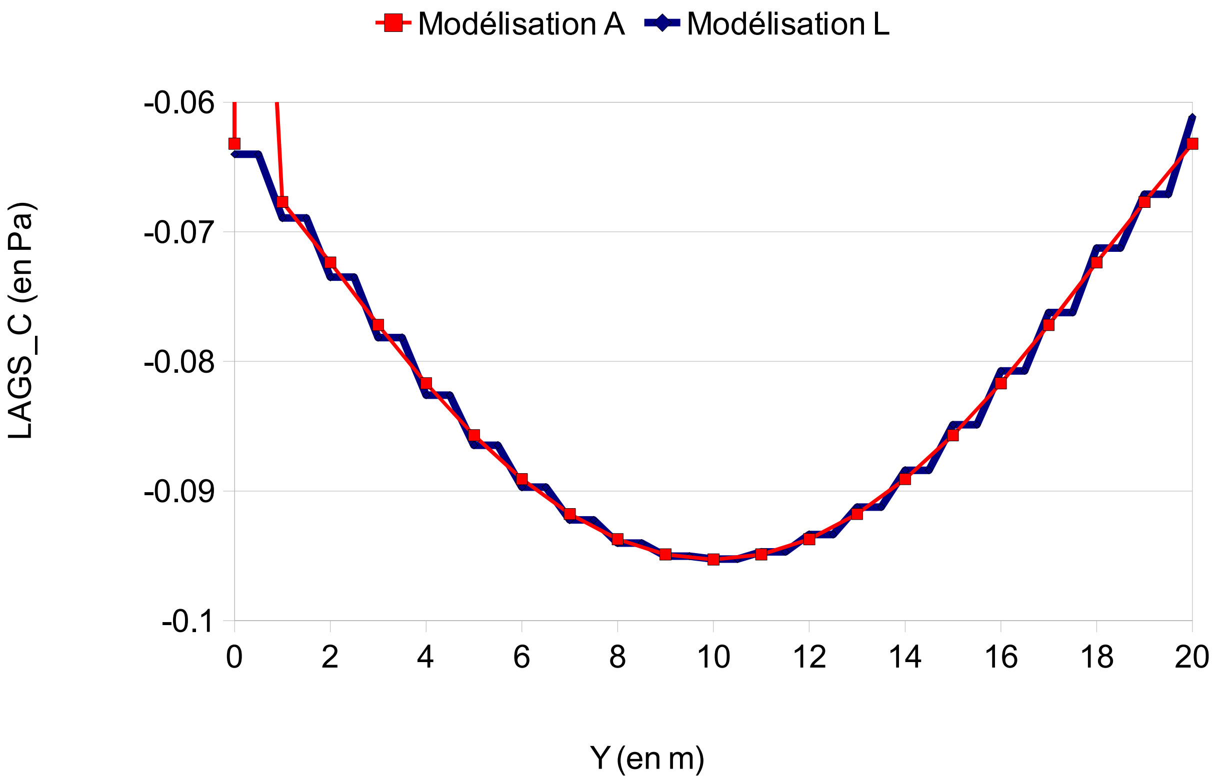


**Figure 14.4-1: Comparison of contact pressures following the modelizations**

## 14.5 Comments

One A finds results comparable to those of the modelization where the unit of the mesh of structure contains hexahedrons. The introduction of the pyramids into the mesh to the level of contact surface deteriorates little the results of contact pressures.